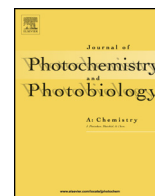




Contents lists available at ScienceDirect

Journal of Photochemistry and Photobiology A: Chemistry

journal homepage: www.elsevier.com/locate/jphotochem

Invited paper

Tuning of photoluminescence properties of functional phthalides for OLED applications



Madhesh Shanmugasundaram^{a,b}, Joshy Joseph, Dr.^{a,b}, Danaboyina Ramaiah, Prof.^{a,b,c,*}

^a Photosciences and Photonics Section, Chemical Sciences and Technology Division, CSIR-National Institute for Interdisciplinary Science and Technology (CSIR-NIIST), Thiruvananthapuram 695019, Kerala, India

^b Academy of Scientific and Innovative Research (AcSIR), CSIR-NIIST Campus, Thiruvananthapuram 695019, Kerala, India

^c CSIR-North East Institute of Science and Technology (CSIR-NEIST), Jorhat 785006, Assam, India

ARTICLE INFO

Article history:

Received 29 May 2016

Received in revised form 4 August 2016

Accepted 6 August 2016

Available online 8 August 2016

Keywords:

Phthalides

Absorption

Fluorescence

Aggregation-induced emission

Organic light emitting diode

ABSTRACT

With an objective to develop simple organic systems and tailor their properties for optoelectronic applications, we have synthesized three functionalized phthalide derivatives and have investigated their electroluminescence and photophysical properties under different conditions. These derivatives showed good solubility in common organic solvents and exhibited strong absorption in the range 320–400 nm, having molar extinction coefficient values of *ca.* $10^4 \text{ M}^{-1} \text{ cm}^{-1}$. The monomeric solution of these derivatives exhibited very low fluorescence quantum yields (Φ_F) of *ca.* 0.003–0.04 owing to their inherent structural features such as intramolecular free rotation and decay to the dark triplet states. However, upon complexation with Lewis acids, such as BCl_3 , these derivatives showed increased fluorescence quantum yields up to *ca.* 0.21 ± 0.01 and also exhibited aggregation induced emission (AIE) in water/acetonitrile mixtures with the emission yields in the range *ca.* 0.11–0.16. The morphological analysis of the aggregates through SEM and TEM showed the formation of rod-like structures in 90% water/acetonitrile mixture with an average size of *ca.* 100 nm. Supporting the observed aggregation induced enhancement in emission properties, these derivatives also exhibited significantly enhanced solid state fluorescence quantum yields of *ca.* 0.58–0.60. As a representative example, organic light emitting diode (OLED) fabricated using the derivative **3** as the emissive layer showed an efficient electroluminescence centered at 524 nm with a turn on voltage of 9 V, demonstrating thereby their potential use in optoelectronic applications.

© 2016 Elsevier B.V. All rights reserved.

1. Introduction

Study of the conjugated organic molecules has been the subject of active research due to their favourable photophysical properties and wide range of applications in organic light-emitting diodes [1–6], non-linear optics [7,8] photovoltaic devices [9–12] and as fluorescent probes [13–20]. Among the various conjugated systems, small organic molecules possess advantages like ease of synthesis and solution processability over macromolecules or inorganic systems [21–23]. However, the applications of such systems in light emitting materials and as fluorescent probes and reporters require tunable luminescence properties [24]. The vast majority of these small organic systems have been known to suffer

from the detrimental effects such as fluorescence quenching due to the free rotation, aggregation induced quenching (ACQ) and decay through dark triplet states resulting in the loss of favourable luminescence properties [24]. One of the approaches adopted to mitigate the effects of various deactivation pathways was through the aggregation induced emission (AIE) phenomenon as proposed by Tang and coworkers [24–26]. These authors have demonstrated through a propeller shaped conjugated molecule, 1-methyl-1,2,3,4,5-pentaphenylsilole, which exhibited aggregation induced high fluorescence intensity due to the restriction of the intramolecular rotation (RIR) of the phenyl substituent [24]. These observations led to the design of interesting AIE active chromophores as luminophores for a variety of applications [25–27]. However, a majority of the reported systems do suffer from issues such as structural complexity, synthetic difficulty and failure in real-time applications. In this context, development of small molecules with tunable excited state and desirable optoelectronic properties are in high demand.

* Corresponding author at: CSIR-North East Institute of Science and Technology (CSIR-NEIST), Jorhat 785006, Assam, India.

E-mail addresses: d.ramaiah@gmail.com, rama@niist.res.in (D. Ramaiah).

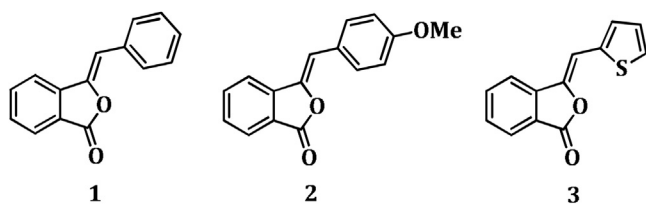


Chart 1. Structures of the phthalide derivatives **1–3** investigated in the present study.

Of the various small molecules investigated, the phthalide (isobenzofuran-1(3H)-one) chromophore has attracted considerable attention in recent years [28–32]. The 3-arylidene phthalide derivatives, in particular, have been used extensively as intermediates for the synthesis of a variety of drugs and photochromic materials [28–33]. Some of the phthalides derivatives were also found to be biologically active as pesticidal, herbicidal, insecticidal, antispasmodic and cytotoxic agents [34–37]. These derivatives exhibited enhanced stability and interesting biological applications compared to the stilbene analogues because of their structural backbone fragment diarylethene connected to an isobenzofuran unit [36–39]. Despite these derivatives are biocompatible, photostable and easy to synthesize, the material applications of such systems have not been explored owing to their radiationless deactivations as a result of the free rotation, intersystem crossing to triplet states and Z-E isomerization [38–40]. Herein, we report the synthesis of the three functionalized phthalide systems **1–3** (Chart 1) and tuning of their luminescent properties through adopting aggregation and Lewis acid complexation approaches. In solution and monomeric state, these derivatives exhibited negligible fluorescence quantum yields. However, upon self assembly in water/acetonitrile mixtures, complexation with Lewis acids such as BCl_3 , and in the solid state, these systems showed significantly enhanced luminescence quantum yields, due to the AIE phenomenon, molecular packing and restricted intramolecular rotation. Uniquely, these small molecular organic systems, showed exceptional thermal and photostability, solution processability and efficient green electroluminescence at 524 nm, thereby indicating their use as optoelectronic materials.

2. Experimental section

2.1. Methods

The melting points were determined on a Mel-Temp II melting point apparatus. The electronic absorption spectra were recorded on a Shimadzu UV-3101 or 2401 PC UV-vis-NIR scanning spectrophotometer. The fluorescence spectra were recorded on a SPEX-Fluorolog F112X spectrofluorimeter. ^1H and ^{13}C NMR were recorded on a 500 MHz Bruker advanced DPX spectrometer. The mass spectra were recorded on a Thermo Scientific Exactive ESI-MS spectrophotometer. Reactions were carried out using MAS-II microwave synthesizer. All the solvents were purified and distilled before use. Quantum yields of fluorescence were determined by the relative methods using optically dilute solutions. Quinine sulphate in 0.1 M H_2SO_4 , with a quantum yield of 0.54 [41], was used as the standard and the quantum yields of fluorescence were calculated using the Eq. (1).

$$\Phi_f = \frac{A_s F_u n_u^2}{A_u F_s n_s^2} \Phi_s \quad (1)$$

wherein A_s and A_u are the absorbance of the standard and unknown, respectively; F_s and F_u are the areas of fluorescence peaks of the standard and unknown, respectively; and n_s and n_u are

the refractive indices of the standard and unknown solvents, respectively. Φ_s and Φ_f are the fluorescence quantum yields of the standard and unknown, respectively.

Photoluminescence quantum yield of the powder samples were measured using a calibrated integrating sphere in a SPEX Fluorolog Spectrofluorimeter. Samples were excited at the absorption maximum using a Xe-arc lamp as the excitation source. The absolute quantum yield was calculated on the basis of the de Mello method [42]. Fluorescence lifetimes were measured on an IBH picoseconds single photon counting system using a 635-nm IBH NanoLED source and a Hamamatsu C4878-02 micro channel plate (MCP) detector. The fluorescence decay profiles were de-convoluted using IBH data station software V2.1, fitted with a mono- or biexponential decay and minimizing the χ^2 values of the fit to 1 ± 0.1 .

Fluorescence microscopic images were obtained using a Nikon HFX 35A Optiphot-2 polarized light optical microscope, equipped with a Linkam THMS 600. Scanning Electron Microscopic (SEM) analysis was performed using drop casted and air dried on flat surface of cylindrical brass stubs and subjected to thin gold coating using JOEL JFC-1200 fine coater, which further was inserted into Zeiss EVO 18 Cryo SCM for taking the images. The Transmission Electron Microscopic (TEM) analysis was performed on JEOL 100 kV high resolution TEM. The compounds were dissolved in acetonitrile to prepare the stock solution. Then by increasing the water percentages of acetonitrile solution up to 90%, we have drop casted on the top of carbon-coated Cu grid. The grids were mounted on reverse tweezers and the samples were dried by a vacuum pump under reduced pressure for 1 h at 25 °C. The accelerating voltage of the TEM was 100 kV and the beam current was 65 A. Samples were imaged using a Hamamatsu ORCA CCD camera.

The organic light emitting device (OLED) was fabricated on glass substrates pre-coated with a layer of indium tin oxide (ITO) having a sheet resistance of 10Ω per square. The ITO substrates were ultrasonically cleaned with detergent, deionized water, acetone and isopropanol, and then dried by blowing nitrogen. A layer of PEDOT:PSS was spin-coated onto the pre-cleaned ITO substrates, and then dried in a vacuum oven at room temperature for 30 min to extract residual water. Then the samples were prepared in a glove box under a nitrogen protected environment (oxygen and water contents less than 1 ppm), and the emissive layers (EMLs) were spin-coated on top of PEDOT:PSS from toluene and then annealed at 120 °C in a vacuum oven for 30 min to remove the residual solvent. Subsequently, the samples were transferred to a thermal evaporator chamber (pressure less than 5×10^{-4} Pa) connected to the glove box without exposure to the atmosphere. 50 nm Tris(8-hydroxyquinoline) aluminium (AlQ_3) [1,43], 1 nm LiF, and 150 nm Al were deposited sequentially by thermal evaporation and then electroluminescence measurements were performed.

2.2. Materials

The starting materials and reagents were purchased from Sigma Aldrich and used without further purification. Spectroscopic grade solvents were purchased from Merck and used as received for photophysical studies. The phthalide derivatives were synthesized through a modified procedure and characterized as described in the Supporting Experimental Section [1, mp 110–111 °C (mixture mp 110–112 °C) [31]; **2**, mp 128–129 °C (mixture mp 128–130 °C) [31]; **3**, mp 113–114 °C (mixture mp 114–115 °C) [31]]. The phthalide- BCl_3 complexes were prepared by dissolving the phthalide derivatives in CH_2Cl_2 and the absorbance of the solution was kept in between 0.3–0.5. Then 50 μL of boron trichloride (BCl_3) solution (1.0 M in CH_2Cl_2) was added to the phthalide solution and

the resultant mixture was allowed to equilibrate for 2 min. The UV–vis absorption, fluorescence emission and other spectral measurements were carried at 25 °C.

3. Results and discussion

3.1. Synthesis and photophysical properties

Synthesis of the phthalide derivatives **1–3** (Chart 1) was achieved in ca. 90–95% yields by one step microwave assisted modified Perkin condensation [29] of phthalic anhydride and the corresponding arylacetic acids (Scheme S1, Supporting information). The products obtained were purified through column chromatography and characterized on the basis of spectral and analytical evidence. The structure of the representative phthalide derivative **3** was further confirmed through single crystal X-ray analysis (Fig. 1). The derivative **3** was found to crystallize in orthorhombic crystal system with Pbc_a space group and have four molecules in its unit cell. Further, the derivative **3** exhibited a unique molecular stacking pattern in such a way that π -stacking is prevented. The molecules are arranged into two non-equivalent stacks (Fig. 1B). The molecules in the first stack were arranged in one plane; however, the molecules in the second stack were packed in a perpendicular plane to the first stack. This unique style of packing allowed the molecules of this phthalide family to show interesting properties.

The phthalide derivatives **1–3** under investigation, showed good solubility in all common organic solvents such as acetonitrile, chloroform, dichloromethane, tetrahydrofuran and ethanol. The absorption and fluorescence spectra of **1–3** in acetonitrile are shown in Fig. 2. These derivatives showed characteristic absorption of the phthalide chromophore and exhibited two structured bands in the region 280–310 nm and 330–380 nm having extinction coefficient values in the range $\sim 10^4 \text{ M}^{-1} \text{ cm}^{-1}$ (Fig. 2A). The derivatives **1** and **2** showed similar absorption spectra with the long wavelength band centered at ca. 335 nm, while the derivative

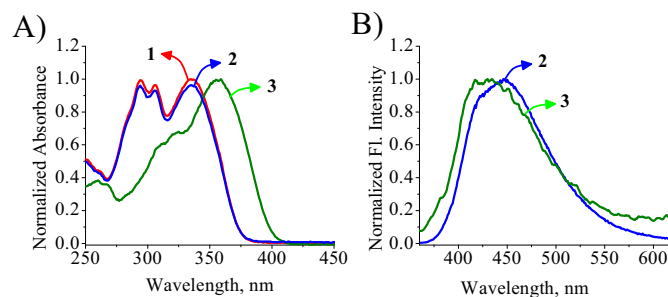


Fig. 2. A) Absorption and B) fluorescence spectra of the phthalide derivatives **1**, **2** and **3** in acetonitrile. $\lambda_{\text{ex}} = 335$ and 360 nm for **2** and **3** respectively.

3 showed a red shifted absorption with a maximum of 355 nm. In the emission spectra (Fig. 2B), all these derivatives showed weak fluorescence in the range 400 nm–600 nm with a maximum at ca. 430 nm and 448 nm, for **2** and **3**, respectively, whereas, the derivative **1** showed negligible fluorescence emission under these conditions. We have determined the fluorescence quantum yields of these systems using quinine sulphate in 0.1 M sulphuric acid as reference ($\Phi_{\text{F}} = 0.54$) [41]. We observed low fluorescence quantum yield values of ca. 4×10^{-2} and 3×10^{-3} for the derivatives **2** and **3**, respectively in acetonitrile. This non-emissive behaviour of these derivatives can be attributed to the predominant non-radiative decay pathways such as free rotation, intermolecular hydrogen bonding and intersystem crossing associated to their structure as reported in the literature [38–40]. The photophysical parameters in the solution state for all the derivatives are summarized in Table 1.

3.2. Aggregation induced emission properties

To understand the propensity of the phthalide systems to undergo aggregation, we have carried out their absorption and emission properties in various mixtures of water and acetonitrile.

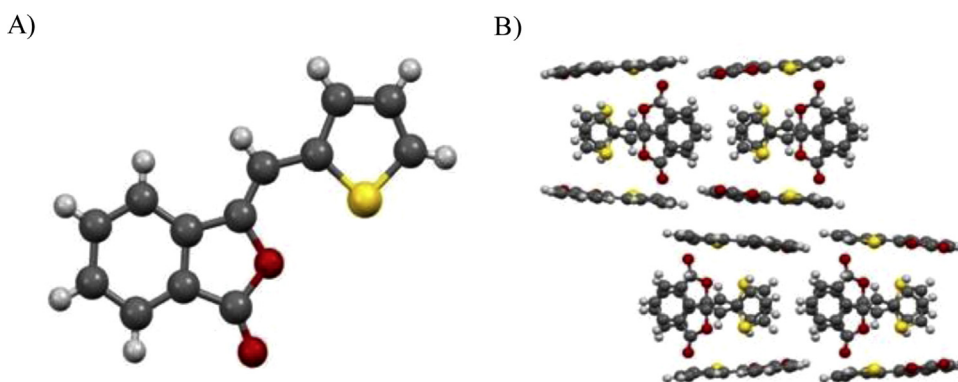


Fig. 1. A) Single crystal X-ray structure showing ORTEP diagram and B) unit cell structure showing the crystal packing of the phthalide derivative **3**.

Table 1
Photophysical properties of the phthalide derivatives **1–3** in solution.^e

Compound	$\lambda_{\text{ab}}^{\text{a,c}}$ (nm)	$\lambda_{\text{abs}}^{\text{b}}$ (nm)	$\lambda_{\text{em}}^{\text{a}}$ (nm)	$\lambda_{\text{em}}^{\text{b}}$ (nm)	$\Phi_{\text{F}}^{\text{a}}$	$\Phi_{\text{F}}^{\text{b}}$
1	335 ($1.9 \pm 0.2 \times 10^4 \text{ M}^{-1} \text{ cm}^{-1}$)	340	^d	432	^d	0.007
2	336 ($3.8 \pm 0.2 \times 10^4 \text{ M}^{-1} \text{ cm}^{-1}$)	337	446	486	0.004	0.21
3	355 ($2.6 \pm 0.1 \times 10^4 \text{ M}^{-1} \text{ cm}^{-1}$)	361	438	478	0.003	0.16

^a Acetonitrile.

^b 90% water-acetonitrile mixture.

^c Molar extinction coefficients are given in parentheses.

^d Negligible emission.

^e Average of more than three experiments, the error is ca. 5%; λ_{abs} = absorption maximum; λ_{em} = emission maximum; Φ_{F} = fluorescence quantum yields.

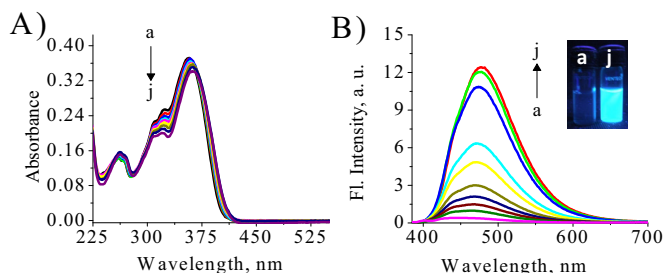


Fig. 3. Changes in A) absorption and B) emission spectra of **3** (15 μM) in various water-acetonitrile mixtures. Percentage of water in acetonitrile (f_w); a) 0 and j) 90%. λ_{ex} 370 nm. The inset shows the visual changes in fluorescence intensity of **3** in acetonitrile and in f_w ca. 90%.

Interestingly, the phthalide derivatives **1–3** showed significant variation in their absorption and emission features with increase in percentage of water in acetonitrile. For example, with an increasing percentage of water in acetonitrile (f_w), we have observed a gradual decrease in the absorbance of the derivative **3** at 355 nm, with a bathochromic shift of 6 nm (Fig. 3A). Similar observations were made for the phthalide derivatives with a bathochromic shift of ca. 5 nm and 6 nm was observed, respectively for **1** and **2**. Further, no intense red shifted peak formation was observed in the absorption spectrum of the phthalide derivatives, which corroborates to the fact that there is negligible probability for the formation of J-type aggregates [44] upon increasing the water content in acetonitrile.

However, in the fluorescence spectrum of the derivative **3**, we observed significant changes with increase in percentage of water (f_w). Upon increasing water fraction from 0 to 90%, we observed ca. 36-fold enhancement of the fluorescence intensity with a bathochromic shift of ca. 40 nm (Fig. 3B). Similar observations were made with the derivatives **1** and **2** (Supporting information, Figs. S1 and S2), wherein we obtained ca. 28-fold and 7-fold enhancement in the fluorescence intensity, respectively. We have calculated the fluorescence quantum yields at 90% of water in acetonitrile and the values are found to be ca. 0.07, 0.21, 0.16 ± 0.01 , for the derivatives **1**, **2** and **3**, respectively. Interestingly, the

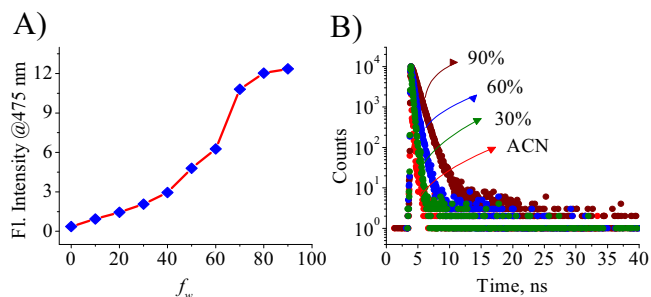


Fig. 5. A) Changes in fluorescence intensity and B) fluorescence decay profiles of **3** (15 μM) monitored at 475 nm, with varying water fraction in acetonitrile (f_w). λ_{ex} 375 nm.

changes in the emission can be visually monitored through the appearance of blue fluorescence emission from colorless for the thiophene derivative **3** under UV illumination with the addition of water as shown in Fig. 4.

Fig. 5A shows the changes in fluorescence intensity of the derivative **3** at 475 nm with variation of water fraction in acetonitrile (f_w). We observed slow increase in intensity initially, but observed significant increase after ca. 50% water fraction in acetonitrile. This clearly suggests the fact that these derivatives undergo molecular aggregation under these conditions, which in turn lead to restriction of the freedom of degree of rotation. As a result we observed increased radiative decay processes and hence fluorescence yields as reported in the literature for several such systems [22–27]. The properties of the systems **1–3** in 90% water-acetonitrile mixture are summarized in Table 1.

To get better insights about the excited state properties of these systems, we have carried out the picosecond time-resolved fluorescence measurements. Fig. 5B shows the fluorescence decay profile of the derivative **3** monitored at 475 nm after the excitation at 375 nm. In acetonitrile, we observed a very short lifetime of <0.01 ns owing to its negligible fluorescence quantum yield. However, by gradually increasing the water fraction to ca. 30%, the derivative **3** decayed bi-exponentially with fluorescence lifetimes of ca. 0.14 ± 0.01 ns (95%) and 0.78 ± 0.02 ns (5%), which can be

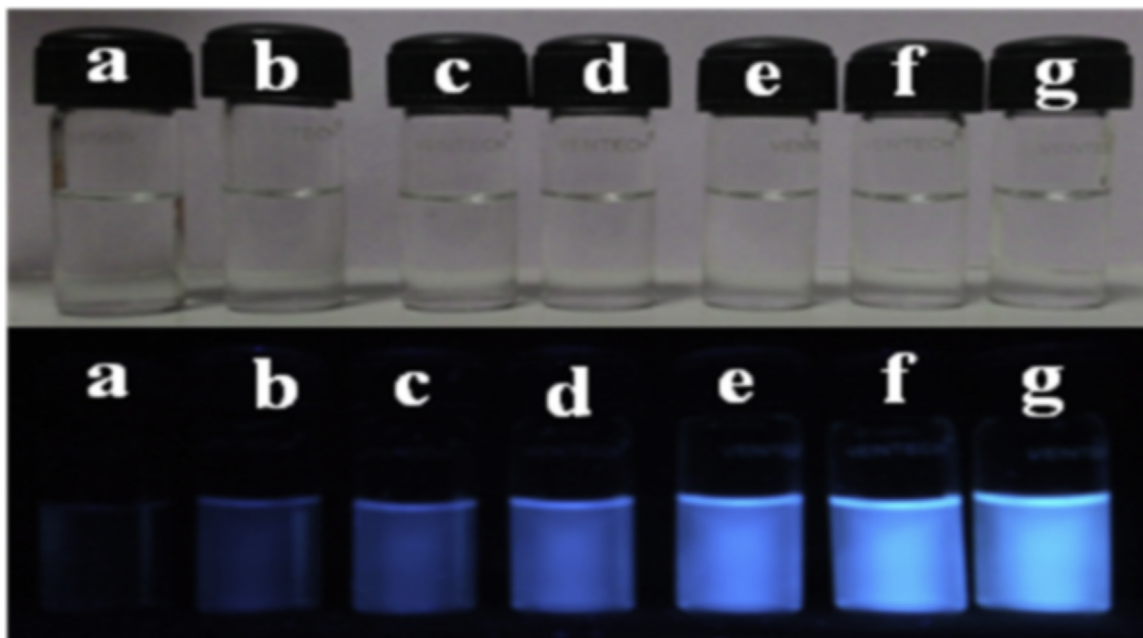


Fig. 4. Photographs showing the visual changes in fluorescence intensity of **3** (15 μM) by varying amounts of water in acetonitrile under normal light (top row) and under UV light (365 nm) (bottom row). Percentage of water (f_w): a) 0, b) 15, c) 30, d) 45, e) 60, f) 75 and g) 90%. λ_{ex} 365 nm.

attributed to the monomer and aggregated species, respectively. On further increase in the water content, the contribution from the long-lived species was found to be increasing with a concomitant decrease in the short-lived species. Interestingly, at *ca.* 90% water-acetonitrile, the conjugate **3** showed monoexponential decay with a fluorescence lifetime value of 0.90 ± 0.01 ns. These results further corroborate the fact that the aggregates formed from these systems are the predominant emitting species present in 90% water-acetonitrile mixture.

With a view to understand the stability of the aggregates formed, we have carried out the temperature dependent studies by employing both UV–vis absorption and fluorescence techniques. At *ca.* 90% water-acetonitrile mixture, the derivative **3**, showed significant quenching of the fluorescence intensity with the increase in temperature from 20 °C to 70 °C (Fig. S3, Supporting information). Notably, in the cooling cycle, from 70 °C to 20 °C, we observed the reverse trend in the emission intensity along with the negligible changes in the absorption spectra. Furthermore, we have investigated the effect of the viscosity on the aggregation properties of these phthalide systems. By varying the amounts of glycerol, a viscous solvent, in ethanolic solution of the derivative **3**, we observed significant enhancement in the emission intensity similar to that of the water-acetonitrile mixtures (Fig. S4, Supporting information). These observations can be attributed to the restriction of the degree of free rotation around the axis of C=C double bond in the phthalide derivatives as reported for similar cases in the literature [22–27].

3.3. Morphological analysis of the aggregates

To understand the nature of the aggregates formed by these systems, we have carried out their morphological analysis through various microscopic techniques such as fluorescence microscopy, scanning electron microscopy (SEM), and transmission electron microscopy (TEM). The fluorescence microscopic images of the derivative **3** showed the formation of rod-like structures in acetonitrile (Fig. 6A) and extended rods in 90% water-acetonitrile mixture (Fig. 6D). This was further confirmed by SEM and TEM analyses under similar conditions, and observed small rod-like structures with an average diameter of *ca.* 30–50 nm in acetonitrile (Fig. 6B and C) and extended rods in 90% water-acetonitrile mixture with an average size of *ca.* 100 nm (Fig. 6E and F).

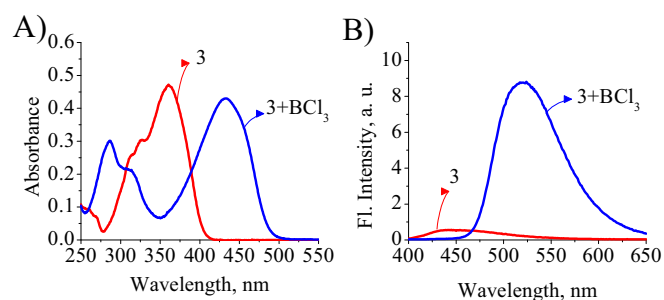


Fig. 7. Changes in the A) absorption and B) fluorescence spectra of the phthalide **3** (15 μ M) with the addition of BCl_3 (16 μ M) in dichloromethane. $\lambda_{\text{ex}} = 390$ nm.

3.4. Interaction with BCl_3

The aromatic ketones generally exhibit weak fluorescence because, the lowest singlet excited states of these systems normally involve $^1(n-\pi^*)$ or $^1(\pi-\pi^*)$ transitions, and undergo rapid intersystem crossing to the dark $^3(n-\pi^*)$ states [45,46]. Interestingly, Zhang and co workers [46–49] have demonstrated that the $^1(n-\pi^*)$ state of these systems can be replaced with a fluorescent singlet charge transfer (^1CT) or $\pi-\pi^*$ excited states by raising the $n-\pi^*$ energy levels of the parent molecule through complexation with Lewis acids. To investigate the effect of Lewis acids, we have monitored the absorption and fluorescence properties of the phthalide derivatives **1–3** with the addition of BCl_3 . For example, the thiophene derivative, **3** initially exhibited absorption band centered at 360 nm and weak emission around 440 nm in dichloromethane (DCM). However, with the addition of BCl_3 (16 mM) in dichloromethane resulted in the formation of new absorption bands centered at 284 and 430 nm with isobestic points at 305 and 390 nm (Fig. 7A). On the other hand, the emission spectrum exhibited significant enhancement with a *ca.* 80 nm bathochromic shift having maximum intensity at *ca.* 520 nm. By the addition of BCl_3 (16 mM), we observed *ca.* 15-fold enhancement in the fluorescence intensity having the quantum yield of *ca.* 0.11 for the complex (Fig. 7B). Similar observations were made for the derivatives **1** and **2** with fluorescence quantum yield values of 0.21 ± 0.01 and 0.18 ± 0.01 , respectively. This formation of a new broad signal in the absorption and enhancement in the fluorescence intensity can be attributed to the formation of a newly

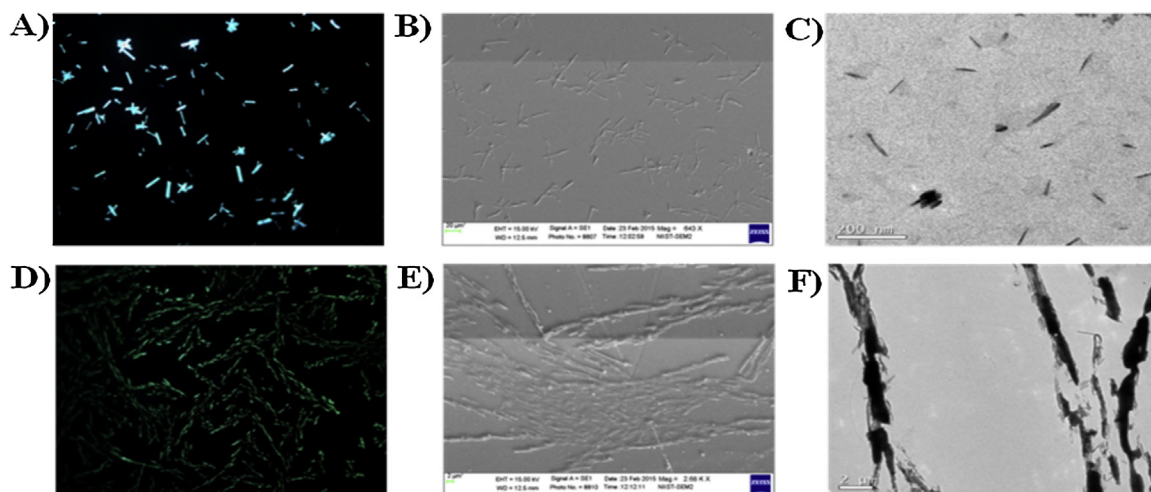


Fig. 6. A) Fluorescence, B) scanning electron (SEM) and C) transmission electron (TEM) microscopic images of the phthalide derivative **3** (100 μ M) in acetonitrile and D)–F) are the corresponding images of the derivative **3** in 90% water-acetonitrile mixture.

generated emissive charge transfer state as reported in the literature [45–49] (Table S2, Supporting information).

3.5. Solid state properties

The aggregation induced emission (AIE) properties exhibited by the phthalide derivatives led us to study their photophysical properties in the solid and thin film states. In this regard, we have monitored the absorption and fluorescence aspects of the compounds in their powder as well as in thin film state. For example, the compound **3** showed bathochromic shifted absorption at around 402 nm, when compared to its absorption (355 nm) in the solution state. On the other hand, it showed significantly enhanced fluorescence intensity centered at 490 nm with a quantum yield value of $ca. 0.54 \pm 0.01$ (Fig. 8) in the powder form. Similar observations were made with the other derivatives, wherein we obtained quantum yield values of $ca. 0.03 \pm 0.01$ and 0.53 ± 0.01 , for **1** and **2**, respectively. Notably, these derivatives showed visible yellowish green luminescence under UV illumination (Fig. S5 and Table S3, Supporting information). In the thin film state, for example, the compound **3** showed absorption at around 403 nm. On the other hand, it showed enhanced fluorescence intensity centered at around 480 nm with a quantum yield value of $ca. 0.60 \pm 0.01$ (Fig. S6 and Table S4, Supporting information). Similar observations were made with the other derivatives, wherein we obtained quantum yield values of $ca. 0.10 \pm 0.01$ and 0.58 ± 0.01 , for **1** and **2**, respectively. The enhanced quantum yields in the powder and thin film state can be explained on the basis of rigidity provided by the solid environment, which prevents the non-radiative relaxations like isomerization and free degree of intramolecular rotation. We have further evaluated the thermal stability of these derivatives using thermo gravimetric analysis by heating samples from 30 to 500 °C (Fig. S7, Supporting information). All the three derivatives **1–3**, exhibited good thermal stability with insignificant weight loss up to 300 °C, with thermal decomposition temperature (T_d) (5% mass loss) of 285, 285 and 390 °C, respectively, which makes them suitable for various optoelectronic applications.

3.6. Organic light emitting diode (OLED) measurements

As the phthalides under investigation showed strong emission in solid state, it was of our interest to demonstrate their ability in real OLED applications. In this regard, we have fabricated a prototype using the compound **3** as the emissive layer. Indium tin oxide (ITO) and aluminium were used as the anode and cathode, respectively. The electroluminescence (EL) spectra of the fabricated light emitting diodes (LED) were recorded by applying voltages in the range of 5–25 V. We observed an increase in the emission intensity with the applied voltage. The electroluminescent spectrum (EL) of the derivative **3** showed emission in the range

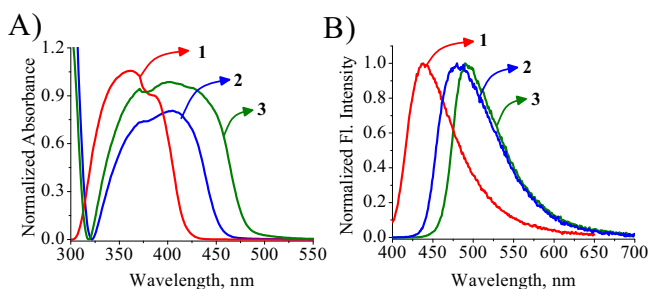


Fig. 8. A) Absorption and B) fluorescence spectra of the phthalide derivatives **1–3** in the solid state. λ_{ex} = 390 nm.

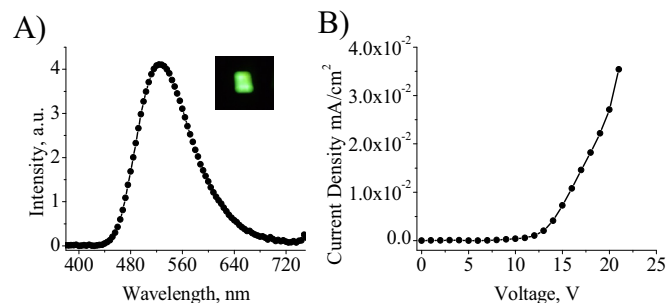


Fig. 9. A) Electroluminescence spectrum of an light emitting diode (LED) device fabricated through spin coating of the solution of the phthalide derivative **3** over an ITO surface. B) Current density–voltage plot of the LED device. The inset shows the visual luminescence of the device.

450–700 nm with a maximum at 524 nm, with a turn on voltage of 9 V (Fig. 9). The EL spectrum showed a red-shift of $ca. 35$ nm, when compared to its solid-state photoluminescence, which can be attributed due to the differences in its molecular packing in the spin coated film and powder. These initial results suggest that these molecules, which can be easily synthesized and show favourable photo physical and electroluminescence properties and can have potential use in optoelectronic applications.

4. Conclusion

In summary, we have synthesized three simple phthalide derivatives **1–3** by employing microwave assisted synthesis and have investigated their photophysical and electroluminescence properties under different conditions. The synthesized molecules exhibited absorption and fluorescence emission in the range 300–400 nm and 400–600 nm, respectively. Interestingly, their fluorescence emission could be tuned from almost non-emissive state in solution ($\Phi_F=0.003$) to a strongly emissive state employing aggregation and Lewis acid coordination and achieved the maximum fluorescence quantum yield in the thin film state ($\Phi_F=0.60 \pm 0.01$). To investigate their utility as light emitting applications, we have fabricated an OLED using the representative derivative **3** as an example, which exhibited efficient green luminescence material with a turn on voltage of 9 V. Our results demonstrate that these simple, thermally stable and solution processable molecular organic systems exhibit favourable photophysical and electroluminescence properties and hence can have potential applications as optoelectronic materials.

Acknowledgments

We acknowledge the financial support from CSIR (CSC 0134 & NWP 55), University Grants Commission (Research Fellowship for MS) and Department of Science and Technology (Ramanujan Fellowship Grant R/JN-19/2012 for JJ), Government of India.

Appendix A. Supplementary data

Supplementary data associated with this article can be found, in the online version, at <http://dx.doi.org/10.1016/j.jphotochem.2016.08.008>.

References

- [1] C.W. Tang, S.A. Vanslyke, Organic electroluminescent diodes, *Appl. Phys. Lett.* 51 (1987) 913–915.
- [2] E. Angioni, M. Chapran, K. Ivaniuk, N. Kostiv, V. Cherpak, P. Stakhira, A. Lazauskas, S. Tamulevicius, D. Volyniuk, N.J. Findlay, T. Tuttle, J.V. Grazulevicius, P.J. Skabara, A single emitting layer white OLED based on exciplex interface emission, *J. Mater. Chem. C* 4 (2016) 3851–3856.

- [3] Y. Sato, S. Ichinosawa, H. Kanai, Operation characteristics and degradation of organic electroluminescent devices, *IEEE J. Sel. Top. Quantum Electron.* 4 (1998) 40–48.
- [4] Y. Lin, Y. Chen, T.L. Ye, Z.K. Chen, Y.F. Dai, D.G. Ma, Oligofluorene-based push-pull type functional materials for blue light-emitting diodes, *J. Photochem. Photobiol. A Chem.* 230 (2012) 55–64.
- [5] K.S. Sanju, D. Ramaiah, White photoluminescence and electroluminescence from a ternary system in solution and a polymer matrix, *Chem. Commun.* 49 (2013) 11626–11628.
- [6] Z. Ning, Y. Zhou, Q. Zhang, D. Ma, J. Zhang, H. Tian, Bisindolylmaleimide derivatives as non-doped red organic light-emitting materials, *J. Photochem. Photobiol. A Chem.* 192 (2007) 8–16.
- [7] D.J. Williams, Organic Polymeric and non-polymeric materials with large optical nonlinearities, *Angew. Chem. Int. Ed.* 23 (1984) 690–703.
- [8] Y. Shi, A.J.T. Lou, G.S. He, A. Baev, M.T. Swihart, P.N. Prasad, T.J. Marks, Cooperative coupling of cyanine and tictoid twisted π -systems to amplify organic chromophore cubic nonlinearities, *J. Am. Chem. Soc.* 137 (2015) 4622–4625.
- [9] L. Han, J. Zhao, B. Wang, S. Jiang, Influence of π -bridge in N-fluorenyl indoline sensitizers on the photovoltaic performance of dye-sensitized solar cells, *J. Photochem. Photobiol. A Chem.* 326 (2016) 1–8.
- [10] J.E. Anthony, Small-molecule, nonfullerene acceptors for polymer bulk heterojunction organic photovoltaics, *Chem. Mater.* 23 (2011) 583–590.
- [11] V. Steinmann, N.M. Kronenberg, M.R. Lenze, S.M. Graf, D. Hertel, K. Meerholz, H. Bürckstümmer, E.V. Tulyakova, F. Würthner, Simple, highly efficient vacuum-processed bulk heterojunction solar cells based on merocyanine dyes, *Adv. Energy Mater.* 1 (2011) 888–893.
- [12] Y. Chen, X. Wan, G. Long, High performance photovoltaic applications using solution-processed small molecules, *Acc. Chem. Res.* 46 (2013) 2645–2655.
- [13] B.H. Shankar, D.T. Jayaram, D. Ramaiah, A reversible dual mode chemodosimeter for the detection of cyanide ions in natural sources, *Chem. Asian J.* 9 (2014) 1636–1642.
- [14] C. Zhang, S. Jin, S. Li, X. Xue, J. Liu, Y. Huang, Y. Jiang, W. Chen, G. Zou, X. Liang, Imaging intracellular anticancer drug delivery by self-assembly micelles with aggregation-induced emission (AIE Micelles), *ACS Appl. Mater. Interfaces* 6 (2014) 5212–5220.
- [15] Y. Liu, Y. Tang, N.N. Barashkov, I.S. Irgibaeva, J.W.Y. Lam, R. Hu, D. Birimzhanova, Y. Yu, B.Z. Tang, Fluorescent chemosensor for detection and quantitation of carbon dioxide gas, *J. Am. Chem. Soc.* 132 (2010) 13951–13953.
- [16] X. Zhang, S. Rehm, M.M. Safont-Sempere, F. Würthner, Vesicular perylene dye nanocapsules as supramolecular fluorescent pH sensor systems, *Nat. Chem.* 1 (2009) 623–629.
- [17] R.R. Avirah, K. Jyothish, D. Ramaiah, Dual-mode semisquaraine-based sensor for selective detection of Hg^{2+} in a micellar medium, *Org. Lett.* 9 (2007) 121–124.
- [18] V.S. Jisha, K.T. Arun, M. Hariharan, D. Ramaiah, Site-selective binding and dual mode recognition of serum albumin by a squaraine dye, *J. Am. Chem. Soc.* 128 (2006) 6024–6025.
- [19] P.A. Gale, C. Caltagirone, Anion sensing by small molecules and molecular ensembles, *Chem. Soc. Rev.* 44 (2015) 4212–4227.
- [20] B.H. Shankar, D. Ramaiah, Dansyl-naphthalimide dyads as molecular probes: effect of spacer group on metal ion binding properties, *J. Phys. Chem. B* 115 (2011) 13292–13299.
- [21] A. Mishra, P. Bäuerle, Small molecule organic semiconductors on the move: promises for future solar energy technology, *Angew. Chem. Int. Ed.* 51 (2012) 2020–2067.
- [22] Y. Hong, J.W.Y. Lam, B.Z. Tang, Aggregation-induced emission, *Chem. Soc. Rev.* 40 (2011) 5361–5388.
- [23] F. Liu, H. Fan, Z. Zhang, X. Zhu, Low-bandgap small-molecule donor material containing thieno [3,4-b] thiophene moiety for high-performance solar cells, *ACS Appl. Mater. Interfaces* 8 (2016) 3661–3668.
- [24] J. Luo, Z. Xie, J.W.Y. Lam, L. Cheng, H. Chen, C. Qiu, H.S. Kwok, X. Zhan, Y. Liu, D. Zhu, B.Z. Tang, Aggregation-induced emission of 1-methyl-1,2,3,4,5-pentaphenylsilole, *Chem. Commun.* (2001) 1740–1741.
- [25] X. Zhang, K. Wang, M. Liu, X. Zhang, L. Tao, Y. Chen, Y. Wei, Polymeric AIE-based nanopores for biomedical applications: recent advances and perspectives, *Nanoscale* 7 (2015) 11486–11508.
- [26] J. Mei, N.L.C. Leung, R.T.K. Kwok, J.W.Y. Lam, B.Z. Tang, Aggregation-induced emission: together we shine united we soar!, *Chem. Rev.* 115 (2015) 11718–11940.
- [27] D.T. Jayaram, S. Ramos-Romero, B.H. Shankar, C. Garrido, N. Rubio, L. Sanchez-Cid, S.B. Gómez, J. Blanco, D. Ramaiah, In vitro and in vivo demonstration of photodynamic activity and cytoplasm imaging through TPE nanoparticles, *ACS Chem. Biol.* 11 (2016) 104–112.
- [28] T. Cheng, Q. Ye, Q. Zhao, G. Liu, Dynamic kinetic resolution of phthalides via asymmetric transfer hydrogenation: a strategy constructs 1,3-distereocentered 3-(2-hydroxy-2-arylethyl)isobenzofuran-1(3h)-one, *Org. Lett.* 17 (2015) 4972–4975.
- [29] J. Safari, H. Naeimi, A.A. Khakpour, R.S. Jondani, S.D.A. Khalili, Rapid and efficient method for synthesis of new 3-arylideneisobenzofuran-1(3h)-one derivatives catalyzed by acetic anhydride under solvent-free and microwave conditions, *J. Mol. Catal. A: Chem.* 270 (2007) 236–240.
- [30] Y.-P. Wang, Y.-L. Wei, C. Dong, Study on the interaction of 3,3-bis(4-hydroxy-1-naphthyl)-phthalide with bovine serum albumin by fluorescence spectroscopy, *J. Photochem. Photobiol. A Chem.* 117 (2006) 6–11.
- [31] S.M. Landge, M. Berryman, B. Török, Microwave-assisted solid acid-catalyzed one-pot synthesis of isobenzofuran-1(3h)-ones, *Tetrahedron Lett.* 49 (2008) 4505–4508.
- [32] I. Cerskus, R.B. Philp, Relationship of inhibition of prostaglandin synthesis in platelets to anti-aggregatory and anti-inflammatory activity of some benzoic acid derivatives, *Agents Actions* 11 (1981) 281–286.
- [33] D. Ramaiah, S. Rajadurai, P.K. Das, M.V. George, Phototransformations of epoxyindanone adducts. steady-state and laser flash photolysis studies, *J. Org. Chem.* 52 (1987) 1082–1089.
- [34] W.-C. Ko, L.-D. Chang, G.-Y. Wang, L.-C. Lin, Pharmacological effects of butylidenephthalide, *Phytother. Res.* 8 (1994) 321–326.
- [35] T. Chamoli, M.S.M. Rawat, A facile synthesis of new 3,3-disubstituted phthalides of pharmacological interest, *Med. Chem. Res.* 22 (2012) 453–465.
- [36] G. Ortari, A.S. Moriello, E. Morera, M. Nalli, V.D. Marzo, L.D. Petrocillis, 3-Ylidene-phthalides as a new class of transient receptor potential channel TRPA1 and TRPM8 modulators, *Bioorg. Med. Chem. Lett.* 23 (2013) 5614–5618.
- [37] D. Rambabu, G.P. Kumar, B.D. Kumar, R. Kapavarapu, M.V.B. Rao, M. Pal, Pd/C-mediated synthesis of (z)-3-alkylidenephthalides of potential pharmacological interest, *Tetrahedron Lett.* 54 (2013) 2989–2995.
- [38] I. Timtcheva, P. Nikolov, N. Stojanov, S. Minchev, Deactivation processes of the excited states of 3-hetarylmethylene-1(3h)-isobenzofuranones in solution: possibility of the formation of intermolecular hydrogen bonds, *J. Photochem. Photobiol. A Chem.* 101 (1996) 145–150.
- [39] P. Nikolov, I. Timtcheva, Photophysical properties of some derivatives of 3-arylmethylene-1(3h)-isobenzofuranone: indication of intermolecular hydrogen-bond formation in the singlet excited state, *J. Photochem. Photobiol. A Chem.* 131 (2000) 23–26.
- [40] H. Dong, C. Hao, J. Chen, J. Qiu, Time-dependent density functional theory study on the hydrogen bonding in electronic excited states of 6-amino-3-((thiophen-2-yl) methylene)-phthalide in methanol solution, *Comput. Theor. Chem.* 972 (2011) 57–62.
- [41] K.T. Arun, D.T. Jayaram, R.R. Avirah, D. Ramaiah, Beta-cyclodextrin as a photosensitizer carrier: effect on photophysical properties and chemical reactivity of squaraine dyes, *J. Phys. Chem. B* 115 (2011) 7122–7128.
- [42] J.C. deMello, H.F. Wittmann, R.H. Friend, An improved experimental determination of external photoluminescence quantum efficiency, *Adv. Mater.* 9 (1997) 230–232.
- [43] G.G. Malliaras, Y. Shen, D.H. Dunlap, H. Murata, Z.H. Kafafi, Nondispersive electron transport in Alq_3 , *Appl. Phys. Lett.* 79 (2001) 2582–2584.
- [44] F. Würthner, T.E. Kaiser, C.R. Saha-Möller, J-aggregates: from serendipitous discovery to supramolecular engineering of functional dye materials, *Angew. Chem. Int. Ed.* 50 (2011) 3376–3410.
- [45] Q. Peng, W. Li, S. Zhang, P. Chen, F. Li, Y. Ma, Evidence of the reverse intersystem crossing in intra-molecular charge-transfer fluorescence-based organic light-emitting devices through magneto-electroluminescence measurements, *Adv. Opt. Mater.* 1 (2013) 362–366.
- [46] X. Zhang, T. Xie, M. Cui, L. Yang, X. Sun, J. Jiang, G. Zhang, General design strategy for aromatic ketone-based single-component dual-emissive materials, *ACS Appl. Mater. Interfaces.* 6 (2014) 2279–2284.
- [47] G. Zhang, R.E. Evans, K.A. Campbell, C.L. Fraser, Role of boron in the polymer chemistry and photophysical properties of difluoroboron-dibenzoylmethane poly(lactide), *Macromolecules* 42 (2009) 8627–8633.
- [48] G. Zhang, J. Chen, S.J. Payne, S.E. Kooi, J.N. Demas, C.L. Fraser, Multi-emissive difluoroboron dibenzoylmethane poly(lactide) exhibiting intense fluorescence and oxygen-sensitive room-temperature phosphorescence, *J. Am. Chem. Soc.* 129 (2007) 8942–8943.
- [49] G. Zhang, S. Xu, A.G. Zestos, R.E. Evans, J. Lu, C.L. Fraser, An easy method to monitor lactide polymerization with a boron fluorescent probe, *ACS Appl. Mater. Interfaces* 2 (2010) 3069–3074.